Recombination kinetics and stability in polycrystalline Cu(In,Ga)Se$_2$ solar cells

W.K. Metzger *, I.L. Repins, M. Romero, P. Dippo, M. Contreras, R. Noufi, D. Levi

National Renewable Energy Laboratory, 1617 Cole Blvd., Golden, CO 80401, United States

ARTICLE INFO

ABSTRACT

Time-resolved photoluminescence (TRPL) measurements indicate that bare Cu(In,Ga)Se$_2$ (CIGS) films degrade when they are exposed to air or stored in nitrogen-purged dry boxes. The degradation significantly affects device performance and electro-optical measurements. Measuring films prior to degradation reveals long lifetimes and distinct recombination properties. For high-quality material, the surface recombination velocity at grain boundaries, bare CIGS surfaces, and CIGS/CdS interfaces is less than 10^3 cm/s, and lifetime values are often greater than 50 ns. In high injection, CIGS has recombination properties similar to GaAs. On completed devices, charge-separation dynamics can be characterized.

© 2008 Elsevier B.V. All rights reserved.

1. Introduction

Cu(In,Ga)Se$_2$ (CIGS) solar cells have achieved efficiencies in excess of 19% [1] and can be processed with a number of potentially cost-effective methods. Hence, CIGS is one of the leading material candidates to displace silicon (Si) in the photovoltaics market. However, a challenge that remains for CIGS research laboratories and industry is to characterize fundamental properties such as carrier concentration and recombination in absorber layers. Without rapid feedback on specific electro-optical properties, it is difficult to distinguish good from bad material, understand performance variations, optimize growth processes, and control this complex quaternary material.

Time-resolved photoluminescence (TRPL) measurements may be able to address certain aspects of this challenge. The technique offers a contactless method to measure recombination in absorber layers. Previous studies have found that the photoluminescence (PL) decay from CIGS absorbers may be described using a double-exponential function

$$I_{PL}(t) = C_1 e^{-t/\tau_1} + C_2 e^{-t/\tau_2}, \tag{1}$$

where $I_{PL}(t)$ represents the PL intensity as a function of time after a fast laser pulse excites carriers in the sample. C_1 and C_2 are coefficients, and τ_1 and τ_2 are decay times that correspond to the initial and final section of the decay curves, respectively. Reported room-temperature values generally extend from several hundred picoseconds to several nanoseconds; values for τ_2 have reached values as large as tens of nanoseconds [2–8]. Most studies have implemented very high injection levels of 1–25 μJ/cm^2 per pulse [2–6,8]; but others

have used a considerably lower injection level of 1–50 nJ/cm^2 per pulse [6,7]. Lifetime measurements on completed devices by several groups have yielded larger PL intensity and/or lifetimes than on the corresponding films, leading researchers to conclude that the deposition of CdS or other films on CIGS reduces surface recombination [5–7,9,10]. This suggests that measurements on films may not be directly related to bulk recombination or final device performance. Several studies have found absorber lifetime to be correlated to device performance [2–4], whereas others have not [6,7].

Previous studies generally do not discuss how samples were handled and if degradation was an issue. Nor do they characterize how recombination varies with injection level, or explain why charge separation by the junction does or does not influence measurements on devices. In this study, our goal was not to correlate a specific growth parameter or process to lifetime and device performance; instead, we explored the general recombination physics of polycrystalline CIGS in solar cells. In this effort, we performed several hundred TRPL measurements on CIGS films, CIGS/CdS films, and devices at different excitation wavelengths, emission wavelengths, and intensity levels on diverse samples that were stored and handled in different ways. We found that degradation, charge separation, and high injection all tend to push τ_1 down to the range of several hundred picoseconds to several nanoseconds. Films measured prior to degradation reveal much longer lifetimes and distinct recombination kinetics.

2. Experiment

CIGS films measuring 7.5×7.5 cm^2 were deposited on glass/Mo substrates using the National Renewable Energy Laboratory (NREL) three-stage co-evaporation process [11,12]. These films were cut into 2.5×3.8 cm^2 pieces or smaller for TRPL measurements and/or device fabrication. Results are presented for films that were grown to a thickness of 2.2 μm, had a compositional grade characteristic of NREL

* Corresponding author.
  E-mail address: Wyatt_Metzger@nrel.gov (W.K. Metzger).

Table 1
The basic material parameters used in the simulations

Bulk properties	ZnO	CdS	CIGS
E_g (eV)	3.3	2.4	1.1–1.2*
χ (eV)	4.7	4.7	4.64–4.74*
n, p (cm^{-3})	n: 10^{18}, 10^{20}	n: 6.0×10^{17}	p: 2×10^{16}
$\varepsilon / \varepsilon_0$	9	10	13.6
μ_e (cm^2/V-s)	25, 6.25	100	200
μ_h (cm^2/V-s)	5, 1.25	25	25
m_e/m_h	0.2/1.2	0.2/0.8	0.09/0.72
Midgap state (cm^{-3})	N_a: 10^{16}	N_a: 10^{16}	
σ_e/σ_h (cm^2)	$10^{-16}/10^{-13}$	$10^{-15}/10^{-12}$	
τ_e/τ_h (ns)			100/0.1**

The rows correspond to bandgap (E_g), electron affinity (χ), electron or hole concentration (n, p), dielectric constant ($\varepsilon/\varepsilon_0$), electron and hole mobility (μ_e, μ_h), [17] midgap-state concentration, electron and hole cross-sections (σ_e, σ_h) in the ZnO and CdS layers, and electron and hole lifetime in the CIGS layer (τ_e, τ_h), respectively. Entries separated by a comma in the ZnO column correspond to intrinsic and doped ZnO, respectively. (*CIGS layer is graded. **Values used, except where stated otherwise.)

high-efficiency devices [11], and efficiencies generally ranging from ~12% to 18%. However, thin films, films with no grading or a reverse grade, and films grown with low deposition temperatures were also examined and found to have similar characteristics. To make devices, CdS layers about 50 nm thick were deposited using the chemical-bath deposition technique. Intrinsic (100-nm) and doped (120-nm) ZnO layers were deposited by RF sputtering on pure and Al$_2$O$_3$-doped ZnO targets, respectively. Metallic grids and a 100-nm MgF$_2$ antireflective coating were deposited by electron-beam evaporation. A GaInP/GaAs/GaInP heterostructure was grown for comparison measurements using metal-organic chemical vapor deposition.

Room-temperature PL decay curves were measured by time-correlated single-photon counting [13]. Photoexcitation was provided by an optical parametric amplifier pumped by the output of a titanium:sapphire laser system with a regenerative amplifier. The standard excitation wavelength was 680 nm; 1064 nm was also used where indicated. The final laser output consisted of a 250-kHz pulse train with a pulse width of several hundred femtoseconds (fs) and a beam diameter of 500 μm. The repetition rate was reduced to 25 kHz for GaAs samples. Unless stated otherwise, the injection level corresponded to ~4×10^{10} photons/cm^2 per pulse (~8 nJ/cm^2 per pulse) and is labeled as I_0. For the measurements reported here, the monochromator was tuned to the PL peak, which occurred at ~1100 nm for most samples.

Numerical TRPL simulations were performed using code written in Sentaurus Device [14]. In each simulation, a 500-fs Gaussian laser pulse injects carriers into CIGS, CdS/CIGS, or ZnO/CdS/CIGS structures with layer thicknesses corresponding to the standard CIGS samples described above. The simulations compute how excess electrons and holes recombine, diffuse, and drift within the sample during and after the laser pulse by solving the Poisson and electron and hole continuity equations with the finite-difference method. The net radiative recombination rate, R_{rad}, as a function of position, $\mathbf{r}$, and time, t, is determined by

$$R_{rad}(t) = B[p(\mathbf{r}, t)n(\mathbf{r}, t) - p_0(\mathbf{r})n_0(\mathbf{r})], \tag{2}$$

where B is the radiative coefficient, p and n are the total free hole and electron densities, and p_0 and n_0 are the equilibrium hole and electron concentrations, respectively. These terms are related by the expressions

$$p = p_0 + \Delta p \tag{3}$$

and

$$n = n_0 + \Delta n, \tag{4}$$

where Δp and Δn are the excess hole and electron densities, respectively. The Shockley–Read–Hall (SRH) recombination rate, R_{SRH}, is modeled with the classic equation

$$R_{srh}(t) = \frac{p(\mathbf{r}, t)n(\mathbf{r}, t) - p_0(\mathbf{r})n_0(\mathbf{r})}{\tau_p(\mathbf{r}, t)\left[n(\mathbf{r}, t) + n_i(\mathbf{r})e^{E_t - E_i/kT}\right] + \tau_n(\mathbf{r}, t)\left[p(\mathbf{r}, t) + n_i(\mathbf{r})e^{E_i - E_t/kT}\right]}, \tag{5}$$

where n_i represents the intrinsic carrier density. E_t represents the energy level of a single trap and is set equal to E_i, which represents the intrinsic energy level. The SRH hole and electron lifetimes are represented by τ_p and τ_n, respectively. Surface recombination and grain-boundary recombination are inserted only when specifically stated. Self absorption and photon recycling [15] effects are not explicitly incorporated into the modeling. A detailed description of the TRPL simulations is given in Ref. [16]. The typical compositional grading of three-stage samples grown at NREL is included in the model [11]. The primary parameters for the constituent materials are listed in Table 1.

For p-type material, p_0 is much larger than n_0, and the total radiative recombination rate (which is proportional to the PL signal) can be rewritten from Eq. (2) as

$$R_{rad}(t) = B\int_V [p_0(\mathbf{r}, t)\Delta n(\mathbf{r}, t) + \Delta p(\mathbf{r}, t)\Delta n(\mathbf{r}, t)]d^3\mathbf{r}. \tag{6}$$

In low-injection conditions ($\Delta n < p_o$), the first term in the integral dominates and the PL intensity tracks the minority-carrier concentration, even if the majority of carriers decay nonradiatively. In high-injection conditions ($\Delta n > p_o$), the second term is more important and the PL intensity tracks the square of the excess carrier concentration.

3. Results and discussion

The decay curves are generally bi-exponential. The lifetime values reported here are determined by fitting a single exponential through the initial section of the decay curve, and hence correspond to τ_1. Fig. 1 illustrates a long decay curve measured at I_0 on a bare CIGS film several minutes after it was removed from the growth chamber. The lifetime is about two orders of magnitude larger than τ_1 values typically reported in the literature. Attaining such a large lifetime requires both outstanding material quality and careful measurements [18].

As soon as bare CIGS films are exposed to air, they begin to degrade. To quantify this effect, samples were measured at different times after being removed from the vacuum chamber. The beam was blocked between measurements and moved to a different spot on the film because the laser light itself has been observed to accelerate degradation. Fig. 2a illustrates the results for a representative sample. In one hour, the lifetime was roughly half its original value. After almost a day, the lifetime decreased by almost a factor of 50 to ~2 ns, a typical literature value.

Samples stored in nitrogen-purged dry boxes also degrade, but more slowly. Fig. 2b illustrates results for a sample that was broken
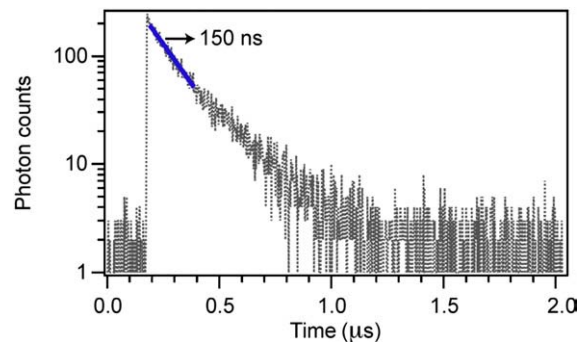

Fig. 1. TRPL data on a CIGS film.